

Template Overlap Method for Massive Jets

Leandro G. Almeida^{a,b}, Seung J. Lee^c, Gilad Perez^c, George Sterman^a, Ilmo Sung^a

^a *C.N. Yang Institute for Theoretical Physics
Stony Brook University, Stony Brook, New York 11794-3840, USA*

^b *Physics Department, Brookhaven National Laboratory
Upton, New York 11973, USA*

^c *Department of Particle Physics and Astrophysics
Weizmann Institute of Science, Rehovot 76100, Israel*

Abstract

We introduce a new class of infrared safe jet observables, which we refer to as template overlaps, designed to filter targeted highly boosted particle decays from QCD jets and other background. Template overlaps are functional measures that quantify how well the energy flow of a physical jet matches the flow of a boosted partonic decay. Any region of the partonic phase space for the boosted decays defines a template. We will refer to the maximum functional overlap found this way as the template overlap. To illustrate the method, we test lowest-order templates designed to distinguish highly-boosted top and Higgs decays from backgrounds produced by event generators. For the functional overlap, we find good results with a simple construction based on a Gaussian in energy differences within angular regions surrounding the template partons. Although different event generators give different averages for our template overlaps, we find in each case excellent rejection power, especially when combined with cuts based on jet shapes. The template overlaps are capable of systematic improvement by including higher order corrections in the template phase space.

1 Introduction

At the Large Hadron Collider, QCD will produce hadronic final states of unprecedented complexity, and most searches for beyond-standard model physics will have to contend with large backgrounds. Over the past few years, scenarios have been proposed in which heavy particles, including the Higgs and top quark, are produced at large transverse momentum [1–11]. At high enough p_T , their decay products will appear as heavy, collimated jets [12, 13]. Even such exotic final states, however, will coexist with a substantial tail of the mass distribution of light-parton QCD jets [14, 15], and it will generally be necessary to study jet substructure systematically to distinguish such a signal.

A number of methods to analyze high- p_T jets have been proposed and tested (so far) against the outputs of event generators. Generally, these methods depend on differences in the substructure of light-parton QCD jets compared to those from particle decays. Diagnostics to detect this difference include infrared safe event shapes [16, 17], and direct analyses of jet substructure [3, 18–23]. To this crowded field we propose a new method, based on a direct quantitative comparison of the energy flow of observed jets at high- p_T with the flow from specific partonic decay modes of boosted heavy particles. Especially when combined with event shape information, the analysis of energy flow provides a potentially powerful tool.

Before going into details, we note that energy flow is a natural language for the description of jet structure. Jet cross sections are naturally described in terms of correlation functions of energy flow [24], which can be interpreted as correlations of the energy-momentum tensor on the sphere “at infinity” [25–28]. For QCD, these correlations tend to be strongly peaked, of course, around jets that may represent the scattering or production of the partons of QCD or the decays of short-lived resonances reflecting new dynamics.

It is interesting to draw a contrast between QCD and the analogous problem for the cosmic background temperature, where the power distribution is very smooth. Indeed, motivated by observation as well as the inflation paradigm one expects for this case a nearly scale invariant, almost featureless, differential power spectrum. Hence, the CMB power spectrum, as well as the microscopic physics of the primordial epoch of inflation, is conveniently described by two and three point correlation functions of the power spectrum in momentum space [29]. Similarly, in case of conformal dynamics, the energy distribution resulting from hard scatterings can be well described by energy-energy correlation functions in momentum space [28], and again is found to be smoothly distributed, almost spherically symmetric. At first sight, energy flow in jet events could not be more different. The search for the origin of a given jet, however, whether from QCD radiation or from decay, may benefit from taking a similar viewpoint, based on the pattern of energy correlations within jets. In this paper, we will present a method for such a quantitative study, with the aim of identifying jets that correspond to resonance decay. We will refer to this as a “template” method, in which we use our knowledge of the signal to design a custom analysis for each resonance, to make use

of differences in energy flow between signal and background.

We can summarize the template overlap procedure as follows. We denote by $|j\rangle$ the set of particles or calorimeter towers that make up a jet, identified by some algorithm, and take $|f\rangle$ to represent a set of partonic momenta $p_1 \dots p_n$ that represent a boosted decay, found by the same algorithm. We will introduce a functional measure $\mathcal{F}(j, f) \equiv \langle j|f\rangle$ that quantifies how well the energy flow of $|j\rangle$ matches $|f\rangle$. Any region of partonic phase space for the boosted decays, $\{f\}$, defines a template. We will often define the template overlap of observed jet j as $ov(j, f) = \max_{\{f\}} \mathcal{F}(j, f)$, the maximum functional overlap of j to a state $f[j]$ within the template region. Template overlaps provide us with a tool to match unequivocally arbitrary final states j to partonic partners $f[j]$ at any given order. Once a “peak template” $f[j]$ is found, we can use it to characterize the energy flow of the state, which gives additional information on the likelihood that it is signal or background.

To make the matching between physical and template possible, each event is characterized by some set of particle or calorimeter energies, $E(\theta_i, \phi_j)_{i,j \in R}$, where E is the energy and θ and ϕ represent coordinates internal to a jet with cone or related parameter R . In a typical experimental setup the energy is discretized according to the detector resolution, and each pair i, j corresponds to a specific cell in the calorimeter. At the LHC experiments [30], for instance, electromagnetic calorimeter cell size (in η and ϕ) is of $\mathcal{O}(0.025 \times 0.025)$ and of $\mathcal{O}(0.1 \times 0.1)$ for hadronic calorimeter cells. For each event, the overlap with the template states is calculated.

In general, for each state j , the template state $f[j]$ with maximal overlap with j will be used to characterize the event j . We therefore adopt the ansatz that a good (if not the best) rejection power is obtained when we use the signal distribution itself to construct our templates (see *e.g.* [29]). At lowest order all the information encoded in the events is matched uniquely to the lowest order template with maximum overlap. After showering and hadronization, this correspondence is diluted, but as we shall see, very meaningful correlations remain.

The application of these ideas is particularly straightforward for top jets. Much of the QCD background is characterized by two sub-jets, with very different energy flow from the three-parton templates in general. Indeed, for a lowest order partonic QCD jet consisting of the original parton plus one soft gluon, there is no template state from top decay that matches the energy flow. This gives a fundamental discrimination, to which we can add additional information from event shapes.

Having given a rationale for the template method, in the following section we provide a general formalism to describe it. In Sec. 3 we apply the method to templates tailored to a boosted top search. In this case, as noted above, the three-particle structure of the lowest-order templates gives a clear distinction between signal and background, which we amplify further by the use of other infrared safe event shapes. Comparisons are carried out using anti- k_T jet finders for events found from several Monte Carlo (MC) generators. In

each case, we find large background rejection powers based on this analysis, with substantial efficiencies.

Highly boosted Higgs decays are discussed in Sec. 4. In this case, the signal and background are both two-parton states at lowest order (LO). Their template overlap distributions are slightly different, but here we use another feature of the template method: the uniqueness of the template state with maximum overlap. This information provides us with an additional, infrared safe tool, which will enable us to attain significant rejection power even in this case. We conclude in Sec. 5.

2 Overlap Formalism

We want our template overlaps to be functionals of energy flow of any specific event (usually involving jets), which we label j , and a model, or template, for the energy flow in a signal, referred to as f . Our templates will be a set of partonic momenta $f = p_1 \dots p_n$, with

$$\sum_{i=1}^n p_i = P, \quad P^2 = M^2, \quad (1)$$

which we take to represent the decay products of a signal of mass M . For example, the lowest-order template for Higgs decay would have $n = 2$ and for top decay, $n = 3$. Of course, templates with more than the minimum number of particles are possible. To represent the sum over this n -particle phase space, we introduce the notation

$$\tau_n^{(R)} \equiv \int \prod_{i=1}^n \frac{d^3 \vec{p}_i}{(2\pi)^3 2\omega_i} \delta^4(P - \sum_{i=1}^n p_i) \Theta(\{p_i\}, R), \quad (2)$$

where the function $\Theta(\{p_i\}, R)$ limits the phase space integral to some region, R , which may represent a specific cone size, for example.

We would like to measure how well the energy flow of any given event j matches that of the signal on the unit sphere, denoted by Ω . We represent the template energy flow as $dE(f = p_1 \dots p_n)/d\Omega$. This function is taken at fixed (to start with, lowest) order. Similarly, we will represent the energy flow of event j as $dE(j)/d\Omega$. This quantity is observed, either in experiment or the output of an event generator. Schematically, a general overlap functional $Ov(j, f)$ is represented as

$$Ov(j, f) = \langle j|f \rangle = \mathcal{F} \left[\frac{dE(j)}{d\Omega}, \frac{dE(f)}{d\Omega} \right]. \quad (3)$$

In principle, the choice of the functional \mathcal{F} is arbitrary.

A natural measure of the matching between state j and the template is the weighted difference of their energy flows integrated over some specific region that includes the template

momenta p_i . To quantify this difference, we construct the functional \mathcal{F} using the template states. We will find it useful to identify the difference in terms of the template configuration in n -particle phase space with the *closest match* of energy flow to a given state j . As a measure of the matching we introduce a function $\Phi(x)$ that is maximized at $x = 0$ to $\Phi(0) = 1$, which represents a “perfect” match. A simple example, which we will employ below, is a Gaussian,

$$Ov^{(F)}(j, f) = \max_{\tau_n^{(R)}} \exp \left[-\frac{1}{2\sigma_E^2} \left(\int d\Omega \left[\frac{dE(j)}{d\Omega} - \frac{dE(f)}{d\Omega} \right] F(\Omega, f) \right)^2 \right], \quad (4)$$

where we introduce a width, σ_E with units of energy. For infrared safety, the function $F(\Omega, f)$ should be a sufficiently smooth function of the angles for any template state f [31]. For example, it could be defined as a Gaussian around each of the directions of the template momenta [32]. Alternately, we may choose F to be a normalized step function that is nonzero only in definite angular regions around the directions of the template momenta p_i [33]. This is the method we will use below. We emphasize that the choice of our overlap functional is to a large extent arbitrary, subject to the requirements of infrared safety. We will find, however, that relatively simple choices can give strong enrichment of signals.

To be specific, for an n -particle final state, we will represent our template overlap (dropping the superscript (F)) as

$$Ov(j, p_1 \dots p_n) = \max_{\tau_n^{(R)}} \exp \left[-\sum_{a=1}^n \frac{1}{2\sigma_a^2} \left(\int d^2\hat{n} \frac{dE(j)}{d^2\hat{n}} \theta(\hat{n}, \hat{n}_a^{(f)}) - E_a^{(f)} \right)^2 \right], \quad (5)$$

where the direction of template particle a is \hat{n}_a and its energy is $E_a^{(f)}$. In applications below, we will use these energies to set the widths of the Gaussians. The functions $\theta(\hat{n}, \hat{n}_a^{(f)})$ restrict the angular integrals to (nonintersecting) regions surrounding each of the template momenta. We will refer to the corresponding state as the “peak template” $f[j]$ for state j . The peak template $f[j]$ provides us with potentially valuable information on energy flow in j .

In summary, the output of the peak template method for any physical state j is the value of the overlap, $Ov(j, f)$, and also the identity of the template state $f[j]$ to which the best match is found. As we shall see, this will be of particular value when we apply our method to boosted Higgs. We turn first, however, to the analysis for boosted tops.

3 Three-particle Templates and Top Decay

In this section, we illustrate the peak template method for top identification, using as a template the LO partonic three-particle phase space of top decay. The essential observation is that light-quark and gluon jets (generally referred to as “QCD jets” below) typically have

states with a two-subjet topology. Such states generally do not match well with a three-particle template, and so are easy to separate from the signal on the basis of their low values of Ov [15, 17]. Of course, some top decay states have low values of Ov also, and some QCD jets higher values. We will see how to combine the template overlap with planar flow to develop a filter that enriches the top signal at relatively high efficiency.

3.1 Peak template overlap method

We begin with a detailed description of the peak template overlap method with the LO three-parton templates appropriate to top jet analysis.

3.1.1 Mass cut and discretization of data

First, we select data using a jet mass window for the top, choosing $160 \text{ GeV} \leq m_J \leq 190 \text{ GeV}$, with top mass chosen to be 174 GeV [§], cone size $R = 0.5$ ($D = 0.5$ for anti- k_T jet algorithm [34] we are using) and jet energy $950 \text{ GeV} \leq P_0 \leq 1050 \text{ GeV}$. In our demonstration, we choose a discretized θ - ϕ plane, with $\Delta\theta = 0.06$ and $\Delta\phi = 0.1$. Then, we can build a table of energy $E(\text{row}_m, \text{column}_n)$, where row_m and column_n are the row and column number corresponding to the discretized θ and ϕ .

3.1.2 Construction of template states

We wish to generate a sufficient number of template states to cover three-particle phase space for top decay, $t \rightarrow b + W \rightarrow b + q + \bar{q}$. Imposing the condition, $(p_q + p_{\bar{q}})^2 = M_W^2$, there are four degrees of freedom. To construct our set of states, we have chosen a brute force method, based on four angles. We take two of these to be the polar and azimuthal angles that define the b and W directions in the top rest frame, defined relative to the direction of the boost from this frame to the lab frame. The remaining two are again polar and azimuthal angles, that define the q and \bar{q} directions, this time relative to the boost axis from the W rest frame to the top rest frame. This method is by no means unique.

By straightforward Lorentz transformations of particle momenta, the four angles identified above determine the energies and directions of the three decay products of the top at LO. We neglect the possible effects of spin and polarization at the particle level in our construction of template states.[¶]

[§]We choose this value for the purpose of demonstration only, and the running of the top mass may be important.

[¶]In [17] it was shown that for boosted two pronged decays, energy flow is very similar for massive spin zero and spin one.

For this investigation, we discretize all four physical angles with a discretization length of 0.1. As for the discretization of the data, we encode two physical angles in terms of row and column number corresponding to the data discretization scheme. A given template consists of a list ($\text{row}_a, \text{column}_a, E_a, a=1,2,3$) for each of three daughter particles of hardronic top (b, q and \bar{q}). We exclude those templates having particles whose polar angles, θ relative to the jet axis, are larger than the cone size R . Also, we impose an energy cut on the templates, removing templates that have an energy less than 10 percent of the maximum energy for a given particle. The number of template states, constructed as above, that pass these cuts is very large, of order three million. We are confident, therefore, that the maximum overlap found with this set is very close to the true maximum. We emphasize that, once generated, the same set of template states is used for all the data.

3.1.3 The template overlap

We next define an overlap between template, $|f\rangle$, and a specific jet energy configuration $|j\rangle$, $\langle j|f\rangle$. Following Eq. (5), we set

$$Ov(j, f) = \max_{\tau_n^{(R)}} \exp \left[- \sum_{a=1}^3 \frac{1}{2\sigma_a^2} \left(\sum_{k=i_a-1}^{i_a+1} \sum_{l=j_a-1}^{j_a+1} E(k, l) - E(i_a, j_a)^{(f)} \right)^2 \right], \quad (6)$$

where $E(i_a, j_a)^{(f)}$ is the energy for the template particle a , whose direction is labelled by indices i_a and j_a , according to the discretization table described above. For our analysis, we fix σ_a (for the a th parton) by that parton's energy,

$$\sigma_a = E(i_a, j_a)^{(f)} / 2. \quad (7)$$

In Eq. (6), we define the overlap between data state j and template f on the basis of an unweighted sum of all the energy in the total of nine cells of state j surrounding (and including) each of the three cells populated by a particle in state f . If one of the cells is located on the edge of the cone in the direction of the polar angle with respect to the jet direction, the number of cells included in the sum is simply taken to be smaller.

3.2 Peak template overlaps for top and QCD jets

We can now apply the peak template function method discussed in the previous sections to analyze energetic top jet events *vis-a-vis* QCD jets. We use the data for QCD jet and hadronic top jet events, for $R = 0.5$, $950 \text{ GeV} \leq P_0 \leq 1050 \text{ GeV}$, $160 \text{ GeV} \leq m_J \leq 190 \text{ GeV}$ and $m_{top} = 174 \text{ GeV}$ as obtained via the anti- k_T jet clustering algorithm [34] with CTEQ6M PDF set [35]. The main purpose of this section is to understand how well we can discriminate our signal from the potentially overwhelming QCD background by using the simplest three-point correlation template functions.

In Fig. 1 we compare the overlap distributions for showered top jets and QCD jets (for the same $z = m_J/P_0$) for event generators Pythia (version 8) [36] for $2 \rightarrow 2$ process without matching, MadGraph/MadEvent (MG/ME) 6.4 [37] (with MLM matching [38] interfaced into Pythia V6.4 [39]), and Sherpa 1.2.1 [40, 41]. It is clear that the showering smears the top distributions significantly, although top events tend to yield somewhat larger peak overlaps. Note also the large variations between the generators.

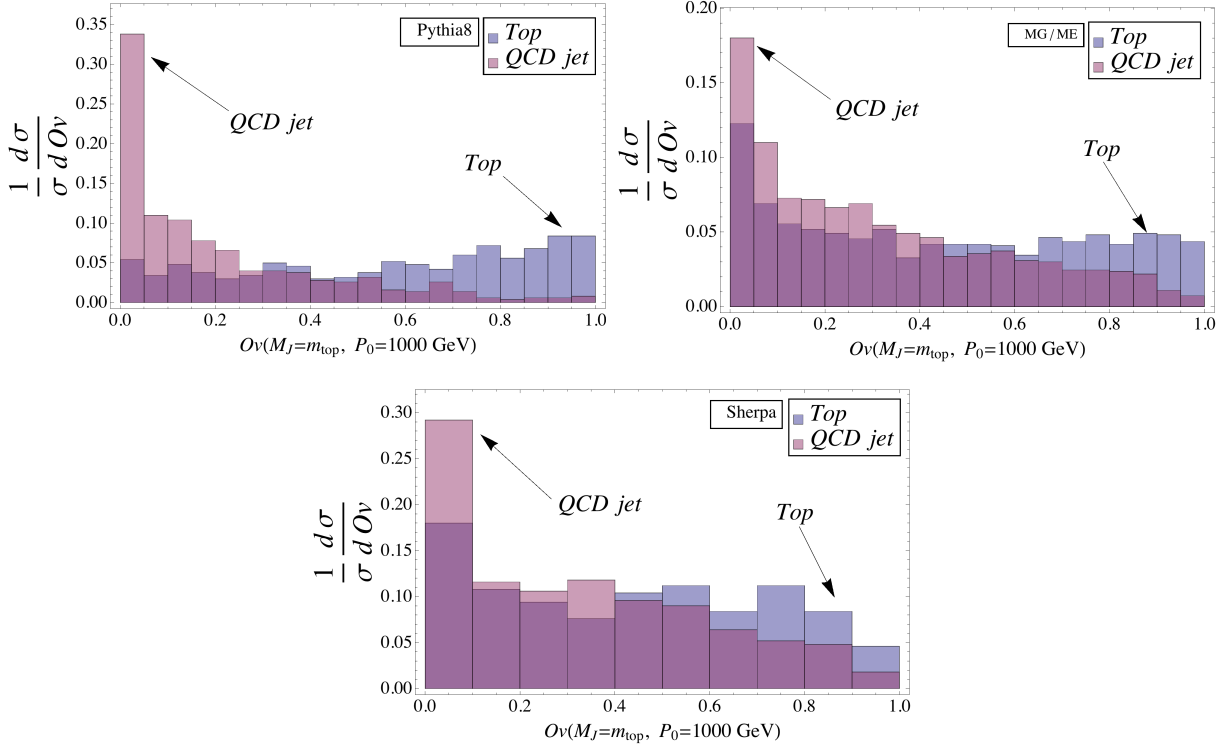


Figure 1: Comparison of histograms of template overlap Ov , Eq. (6), with top jets and QCD jets from different MCs [upper left (right) Pythia (MG/ME) and Sherpa on the bottom], for $R = 0.5$, $950 \text{ GeV} \leq P_0 \leq 1050 \text{ GeV}$, $160 \text{ GeV} \leq m_J \leq 190 \text{ GeV}$ and $m_{top} = 174 \text{ GeV}$.

3.3 Planar flow

We have seen that LO top templates already distinguish noticeably between top and QCD jets. There is still a close relation, with both distributions being fairly flat. To gain a better resolution between the two possibilities, we shall rely on the jet shape variable, planar flow [16, 17]. For completeness we give the definition of the planar flow variable, Pf . First construct for a given jet, a matrix I_ω as

$$I_\omega^{kl} = \frac{1}{m_J} \sum_i \omega_i \frac{p_{i,k}}{\omega_i} \frac{p_{i,l}}{\omega_i}, \quad (8)$$

where m_J is the jet mass, ω_i is the energy of particle i in the jet, and $p_{i,k}$ is the k^{th} component of its transverse momentum relative to the axis of the jet’s momentum. The Pf variable is defined as

$$Pf = \frac{4 \det(I_\omega)}{\text{tr}(I_\omega)^2} = \frac{4\lambda_1\lambda_2}{(\lambda_1 + \lambda_2)^2}, \quad (9)$$

where $\lambda_{1,2}$ are the eigenvalues of I_ω . We shall see that planar flow distinguishes between many three-jet events with large template overlaps. In general, QCD events with large Ov will have significantly smaller planar flow than top decay events. For the QCD jets a large overlap would be a result of a kinematic “accident”. In the studies we show below, the combination of Ov and Pf gives a strong background (QCD) suppression with quite substantial signal (top decay) efficiency.

In Fig. 2, we test these ideas by plotting the template overlap Ov for the partonic level output of a MC, versus Pf . The data shows a scatter plot of Ov and Pf found in this way. The data are all close to unity in Ov , but are (as expected) spread out in planar flow. As we may conclude by looking back at Fig. 1, the effect of showering is to spread out top decays over the full range of Ov .

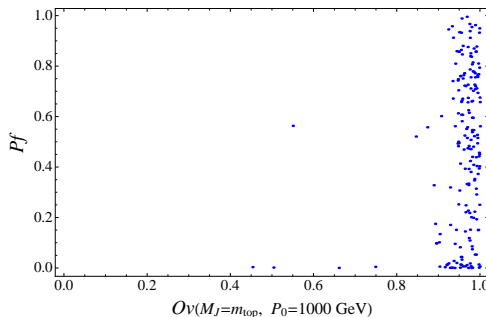


Figure 2: A scatter plot of template overlap, Eq. (6) and Pf for LO parton-level MC output for top quark decay, with $P_0 = 1 \text{ TeV}$, $m_{top} = 174 \text{ GeV}$.

3.4 Application to top decay

In Fig. 3 we show a comparison of scatter plots of planar flow, Pf vs. template overlap, Ov with QCD (first column) top jets (second column) from different MC (from top to bottom: Pythia, MG/ME, Sherpa), for $R = 0.5$, $950 \text{ GeV} \leq P_0 \leq 1050 \text{ GeV}$, $160 \text{ GeV} \leq m_J \leq 190 \text{ GeV}$ and $m_{top} = 174 \text{ GeV}$. The three event generators provide rather different distributions, but in each case the distinction between the signal and background distributions is evident. Clearly, any set of events chosen from the upper right of these plots, with $Pf > Ov$, is highly enriched in top events compared with background. The clear differences in these scatter plots show the potential of the template overlap method.

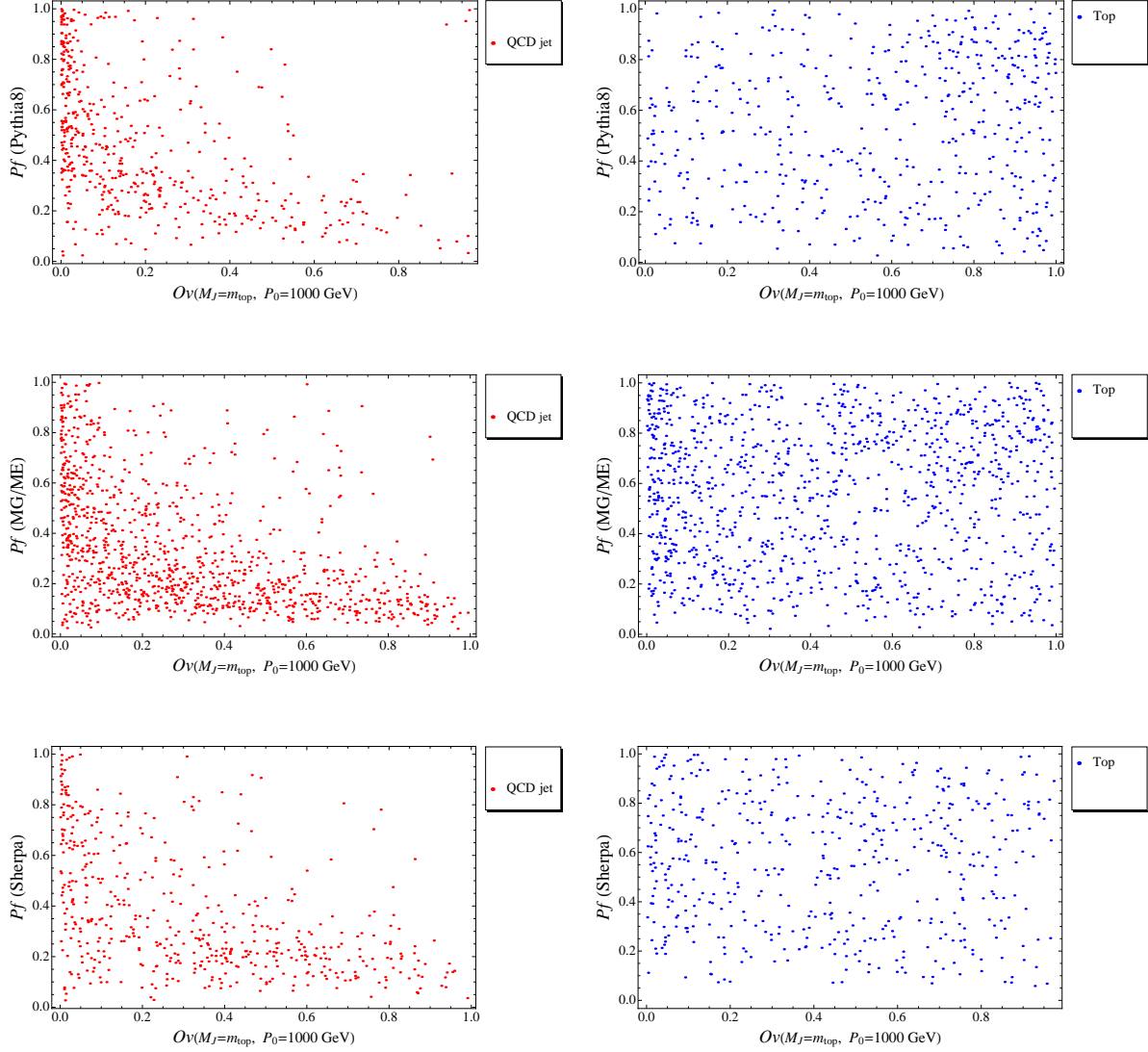


Figure 3: Comparison of scatter plots of planar flow Pf vs. template overlap Ov for top jets (right) and QCD jets (left) from different MC (from top to bottom: Pythia, MG/ME, Sherpa), for $R = 0.5$, $950 \text{ GeV} \leq P_0 \leq 1050 \text{ GeV}$, $160 \text{ GeV} \leq m_J \leq 190 \text{ GeV}$ and $m_{top} = 174 \text{ GeV}$.

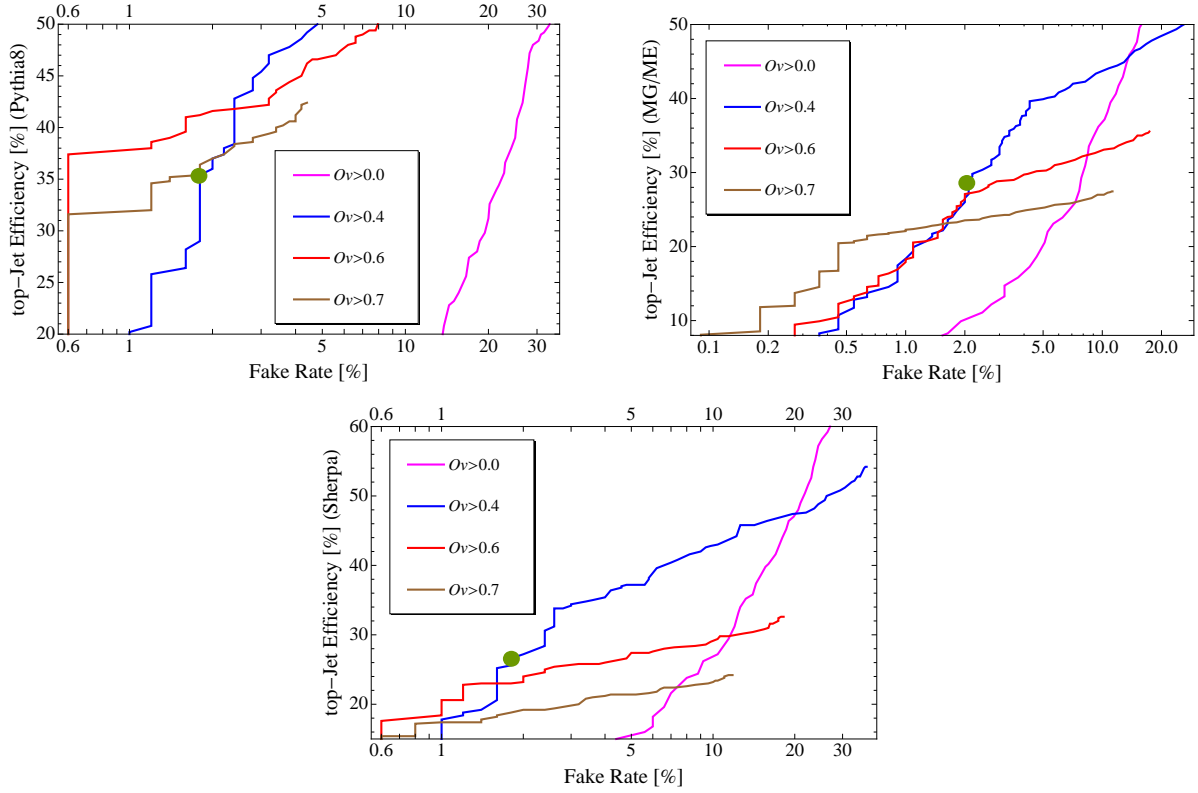


Figure 4: Comparison of fake rate *vs.* efficiency with various cuts on template overlap Ov and Pf with top jets and QCD jets from different MC [upper left (right) Pythia (MG/ME) and Sherpa on the bottom], for $R = 0.5$, $950 \text{ GeV} \leq P_0 \leq 1050 \text{ GeV}$, $160 \text{ GeV} \leq m_J \leq 190 \text{ GeV}$ and $m_{top} = 174 \text{ GeV}$. The lines show the effect of cuts in planar flow (Pf) for fixed overlap (Ov), with the lowest (most inclusive) Pf cuts to the right. The green dot is for $Pf > 0.6$ and $Ov > 0.4$.

As a simple application of these ideas, in Fig. 4, we show fake rate *vs.* efficiency with various cuts on the template overlap Ov as found from Fig. 3. For a given cut on Ov denoted by a same-colored line, the efficiency is controlled by the upper cut on Pf . Each point on one of these curves corresponds to a specific choice of Pf at fixed Ov , and hence to the set of points within a rectangle that includes the upper right corners of the corresponding scatter plots in Fig. 3. The results depend on the choice of Ov cut, but it is clear that any cut above 0.2 leads to a substantial increase in efficiency. We present these results for demonstration purposes only, and have not carried out a systematic study of how to maximize rejection power.

Our final results for the top jet case are summarized in Table 1 for the three different event generators, chosen for the best working point found by these simple, naive one-dimensional cuts in Ov and Pf . It is evident from the numbers presented that the template overlap method works well for events generated by any of the MC generators. In each case, we find a large enhancement of signal compared to background, typically of the order of fifteen or more. Taking into account the rejection of QCD jets by imposing a mass window, these numbers (for a single massive jet) are multiplied by factors of ten to twenty. The template-based approach thus yields numbers that compare favorably with those found from other methods in the literature (see for example table 9 of Ref. [42]). In addition, it allows for systematic improvement, for example by incorporating the effect of gluon emission in the template, or by weighting phase space by squared matrix elements. Because the template method naturally provides scatter plots like those in Fig. 3, we can imagine optimizing cuts on the data. We may also investigate improvements in the overlap functional Eq. (6).

Finally, we note that it is evident both from the scatter plots in Fig. 3 and the efficiency distributions in Fig. 4 that the different generators tend to yield different energy flow patterns. In particular, the green dots on each of the three plots are the result of identical cuts over Ov and Pf . This was also noted earlier in the context of the jet mass distribution [15]. This observation should serve as a caution regarding the interpretation of tests for all methods, especially those that rely heavily on the anticipated structure of soft radiation in final states.

4 Two-particle Templates and Higgs Decay

We now apply the template overlap method to boosted Higgs boson decays. The following discussion applies as well to electroweak bosons, because spin produces relatively small effects in the energy flow [17]. We define the leading order templates in terms of the lowest-order decays of the Higgs, schematically,

$$|f\rangle = |h\rangle^{(\text{LO})} = |p_1, p_2\rangle. \quad (10)$$

MC	Jet mass cut only		Mass cut + $ Ov + Pf $	
	Top-jet efficiency [%]	fake rate [%]	Top-jet efficiency [%]	fake rate [%]
Pythia8	58	3.6	21	0.022
MG/ME	52	3.7	11	0.017
Sherpa	34	3.2	7	0.032

Table 1: Efficiencies and fake rates for jets with $R = 0.5$ (using anti- k_T : $D = 0.5$), $950 \text{ GeV} \leq P_0 \leq 1050 \text{ GeV}$, $160 \text{ GeV} \leq m_J \leq 190 \text{ GeV}$ and $m_{top} = 174 \text{ GeV}$. The left pair of columns shows efficiencies and fake rates found by imposing the jet mass window only. The right pair takes into account the effects of cuts in Ov and Pf in addition to the mass window. For the different MC simulations, we have imposed various cuts on Ov and Pf variables: for Pythia8 $Ov \geq 0.6$ and $Pf \geq 0.4$, for MG/ME $Ov \geq 0.7$ and $Pf \geq 0.39$ and for Sherpa $Ov \geq 0.6$ and $Pf \geq 0.48$.

As above, our template will be a set of discretized partonic states corresponding to given angular configurations.

The task of disentangling a Higgs signal from a QCD background is actually more challenging than for the top, because at lowest order both boosted Higgs and QCD jets consist of two particles. Nevertheless, looking only at the information given from the calorimeter, we can still obtain the measured energy distribution, $dE(j)/d\Omega$, and compare it to templates by an overlap function analogous to Eq. (5). At lowest order, signal phase space for the Higgs is characterized by particularly simple kinematic parameters. For example, in boosted two-particle Higgs decays, $h \rightarrow b\bar{b}$, we can characterize the final state at fixed P_0 by the angle, θ_s between the (two-particle) jet axis and the softer of the two particles. At fixed $z = m_J/P_0 \ll 1$, the distribution in θ_s is given by a “jet” function [17],

$$\frac{dJ^h}{d\theta_s} \propto \frac{1}{\theta_s^3}, \quad (11)$$

rather strongly peaked for small $\theta_s \gg z$. When θ_s approaches its minimum value, the decays are “democratic”, sharing the energy of the Higgs nearly evenly between the pair. The distribution for lowest-order QCD events is still peaked, but much less so [17],

$$\frac{dJ^{\text{QCD}}}{d\theta_s} \propto \frac{1}{\theta_s}. \quad (12)$$

The two-particle phase space parameter θ_s , of course, is not a physical quantity. We can, however, parameterize the two-particle peak template state, $f[j]$ that a physical state, j most closely resembles, by matching energy flows, as discussed in Sec. 2. Once we have identified $f[j]$, we can assign a value of θ_s , or any other kinematic parameter of $f[j]$, to the corresponding physical state j . Template overlaps enable us to make this identification, and therefore to make selections among data events based on quantifiable criteria. In what follows, we apply the peak overlap method introduced in Sec. 2 to Higgs decay.

4.1 Higgs templates

We now describe the procedure for applying the peak template overlap method for Higgs, with a scheme for discretizing the data.

4.1.1 Discretization of the data with jet mass and energy selection

Given a set of data, we impose a jet mass window for the Higgs with a specific cone size R and discretize the data with a convenient mass and energy range: for our demonstration we choose the jet mass window to be $110 \text{ GeV} \leq m_J \leq 130 \text{ GeV}$, with Higgs mass chosen to be 120 GeV , cone size $R = 0.4$ and jet energy $950 \text{ GeV} \leq P_0 \leq 1050 \text{ GeV}$. (For a full analysis, one can discretize the data with a certain step of energy, say 100 GeV , since jet energy is an input of our template function.) This gives us a set of final states j .

For any state j , we determine the measured (or MC generated) energy distribution, $dE(j)/d\Omega$, in the physical θ - ϕ plane with respect to the jet axis for each reconstructed jet, and we can start discretizing data into a jet-energy configuration. In our demonstration for the Higgs, we discretize the θ - ϕ plane into cells of size $\Delta\theta = 0.04$ and $\Delta\phi = 0.1$. Next, we again assemble a table of energies $E(\text{row}_m, \text{column}_n)$, where row_m and column_n are the row and column number corresponding to the discretized values of θ and ϕ .

4.1.2 Construction of template function

As for top decay, we generate our templates f from a set of discretized angles. For the two-body Higgs decay, two angles define the two-body state of the daughter particles. By analogy to the top case, we choose these as the polar and azimuthal angles in the Higgs rest frame, relative to the boost axis that links the Higgs rest frame with the lab frame. A simple Lorentz transformation determines the momenta of the daughter particles in the lab frame, where they are compared to data.

Once again, we generate a large set of template states, so that we are confident of identifying the peak value of overlap. We discretize the angles with a small length of $2\pi/120$.^{||} We can now encode the two physical angles in terms of row and column numbers, corresponding to the data discretization scheme. Each template consists of the information ($\text{row}_a, \text{column}_a, E_a$) for each of the two daughter particles. We exclude those templates having polar angles larger than the cone size R . Also, if desirable, we impose an energy cut on the template, *i.e.*, removing templates with less than five percent of the total energy.

^{||}In fact, one can make it as small as one desires, since we will choose only one of them corresponding to “peak” template.

4.1.3 Two-particle template overlap

We are now ready to implement Eq. (5) for the Higgs, by defining an overlap between templates, $|f\rangle$, and jet states $|j\rangle$, $Ov = \langle j|f\rangle$. Defined as above, our templates each have two cells corresponding to two daughter partons (q and \bar{q}) with their row and column numbers determined by the data discretization scheme.

As for the top, we compute the overlap between data state j and template f from an unweighted sum of all the energy in the total nine cells of state j surrounding and including the two occupied cells of template state f . In summary, we define the overlap of a template function with the energy distribution of the data to be

$$Ov(j, f) = \max_{\tau_n^{(R)}} \exp \left[- \sum_{a=1}^2 \frac{1}{2\sigma_a^2} \left(\sum_{k=i_a-1}^{i_a+1} \sum_{l=j_a-1}^{j_a+1} E(k, l) - E(i_a, j_a)^{(f)} \right)^2 \right], \quad (13)$$

where $E(i_a, j_a)^{(f)}$ is the energy in the template state for particle a . If one of the sums extends outside the jet cone, we set the corresponding energies $E(k, l)$ to zero. Again, we fix σ_a (for the a th parton) by that parton's energy, $\sigma_a = E(i_a, j_a)^{(f)}/2$, as in Eq. (7).

In Fig. 5, we use the overlap, Eq. (13) to validate the template function when compared to MC output events at partonic level, showing that each peak value is close to unity for all the events in our Higgs decaying into a $b\bar{b}$ sample. The points cluster even closer to unity for the Higgs than for the top, Fig. 2, because we have used a finer discretization for the (simpler) Higgs templates.

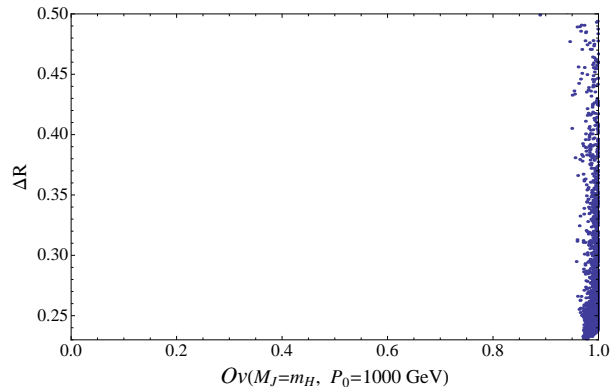


Figure 5: A scatter plot of template overlap, Eq. (13) and the angular distance ΔR between the two partons coming from the Higgs decay, with $P_0 = 1 \text{ TeV}$, $m_H = 120 \text{ GeV}$.

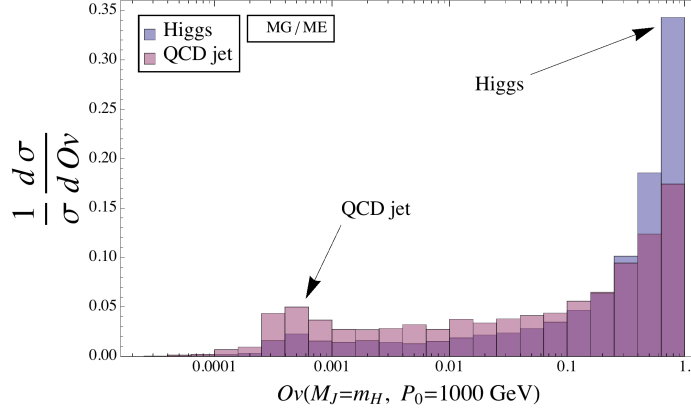


Figure 6: Histogram of template overlap distributions (Eq. (13)) $Ov(j, f_2)$ with MC-generated Higgs jets and QCD jets, where $R = 0.4$, $950 \text{ GeV} \leq P_0 \leq 1050 \text{ GeV}$, $110 \text{ GeV} \leq m_J \leq 130 \text{ GeV}$ and $m_H = 120 \text{ GeV}$. (MG/ME [37] with MLM matching [38].)

4.2 Enhancing overlap with θ_s and angularities

We now apply the peak template overlap method to analyze energetic Higgs jet events *vis-a-vis* QCD jets. We use the data for QCD jet and hadronic Higgs jet events (after showering and hadronization), for $R = 0.4$, $950 \text{ GeV} \leq P_0 \leq 1050 \text{ GeV}$, $110 \text{ GeV} \leq m_J \leq 130 \text{ GeV}$ and $m_H = 120 \text{ GeV}$ as obtained from MG/ME [37] (with MLM matching [38]) via anti- k_T jet clustering algorithm [34].

Our aim is to understand how well we can discriminate our signal from the QCD background using the simplest two-particle templates. In Fig. 6, we compare the template overlap $Ov(j, f)$ distributions from Eq. (13) for Higgs and QCD jets. We see that Higgs jet events are peaked toward larger values of template overlap, Ov than QCD jets. We can therefore use a large Ov value as a quality cut, to ensure that the events under consideration are two-pronged like in terms of the energy flow, say, $Ov \geq 0.85$. Furthermore, even within the two-body description, we have seen that Higgs events tend to be peaked towards smaller θ_s than the QCD jets. We hence expect to improve rejection power from an appropriate cut on θ_s .

To the extent that the energy flow of the jets is similar to that of two-body decay, their kinematics is determined by a single continuous variable, of which θ_s is only one example. Indeed, we can use properties of the data itself as alternatives to θ_s . A set of such alternatives is given the class of angularities, classified by a parameter a and defined by [17, 43]

$$\tilde{\tau}_a(R, m_J) = \frac{1}{m_J} \sum_{i \in jet} \omega_i \sin^a \left(\frac{\pi \theta_i}{2R} \right) \left[1 - \cos \left(\frac{\pi \theta_i}{2R} \right) \right]^{1-a} \sim \frac{1}{m_J} \frac{1}{2^{1-a}} \sum_{i \in jet} \omega_i \left(\frac{\pi \theta_i}{2R} \right)^{2-a}, \quad (14)$$

where ω_i is the energy of a component inside the jet (such as a calorimeter tower). Limiting the parameter $a \leq 2$ ensures IR safety, as can be seen from the second expression on the right-hand side of the equation, which is valid for small angle radiation $\theta_i \ll 1$.

Angularities, $\tilde{\tau}_a$, distinguish between Higgs and QCD jets in much the same way as the template angle θ_s , as can be seen by examining the jet differential distributions in $\tilde{\tau}_a$, analogous to Eqs. (11) and (12) for θ_s . In particular, a simple approximation can be obtained when $z = m_J/P_0 \ll \theta_s \ll 1$ and a is negative with $|a| = \mathcal{O}(1)$,

$$\frac{dJ^h}{d\tilde{\tau}_a} \propto \frac{1}{|a| (\tilde{\tau}_a)^{1-\frac{2}{a}}}, \quad (15)$$

rather strongly peaked for small $\tilde{\tau}_a$. As suggested above, these decays are “democratic”, sharing the energy of the Higgs rather evenly between the pair. The distribution for lowest-order QCD events is still peaked at small $\tilde{\tau}_a$, but less so,

$$\frac{dJ^{\text{QCD}}}{d\tilde{\tau}_a} \propto \frac{1}{|a| \tilde{\tau}_a}. \quad (16)$$

We may thus expect that cuts of the data based on angularities will give results qualitatively similar to those based on θ_s . On the other hand, θ_s , which is a parameter for two-body template states, already provides useful information on physical states, as well as a clear picture of their energy flow.

We now analyze the effects of limiting the data to small θ_s or small angularity. In the plot on the left of Fig. 7, we compare the θ_s distributions for Higgs and QCD jets, with a lower cut of template overlap $Ov \geq 0.85$, which confirms our understanding from Eqs. (11) and (12). A cut $\theta_s \leq 0.2$ (or a corresponding cut on angularity) clearly removes a larger proportion of QCD jets than Higgs jets. In Fig. 8, we show efficiency *vs.* fake rates with various cuts on template overlap Ov . The curves correspond to a variation of the maximum size of the θ_s template parameter cut. Each is a scan from θ_s^{min} (which is fixed by the kinematics) to $\theta_s^{\text{max}} \leq 0.43$. For a given cut on Ov , the efficiency is controlled by the θ_s^{max} variable.

4.3 Planar flow for the Higgs

So far, we have analyzed Higgs jets using only template overlaps based on LO partonic decay kinematics. In principle, the templates can be systematically improved by including the effects of gluon emissions, which contain color flow information [44, 45]. Actually, the effects of higher-order effects can be partly captured by using planar flow [17], which we have already introduced for the top, and defined in Eq. (9). We expect soft radiation from the boosted color singlet Higgs to be concentrated between the b and \bar{b} decay products. This is to be contrasted to a jet initiated by a light parton, whose color is correlated with particles in other parts of phase space, producing radiation in the gaps between those particles and

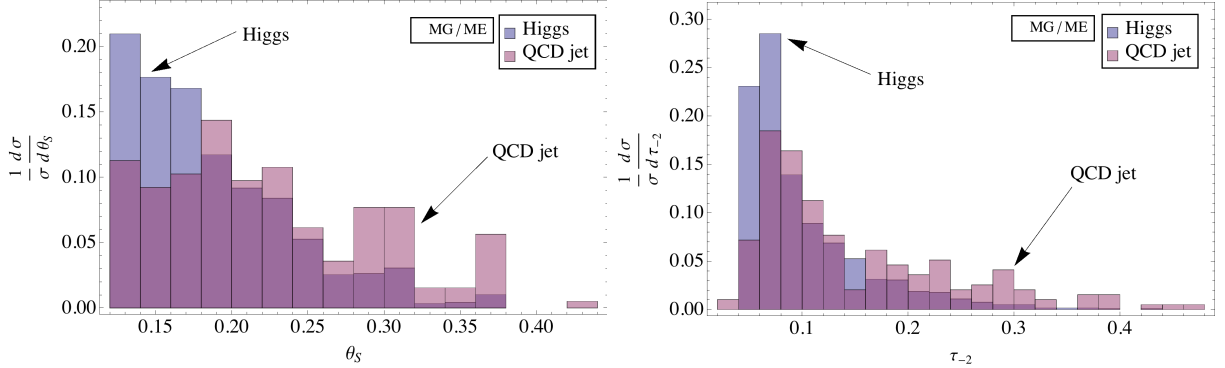


Figure 7: In the plot on the left (right), we show a histogram of θ_s ($\tilde{\tau}_{-2}$) with template overlap $Ov \geq 0.85$. We choose $R = 0.4$, $950 \text{ GeV} \leq P_0 \leq 1050 \text{ GeV}$, $110 \text{ GeV} \leq m_J \leq 130 \text{ GeV}$ and $m_H = 120 \text{ GeV}$. (MG/ME [37] with MLM matching [38].)

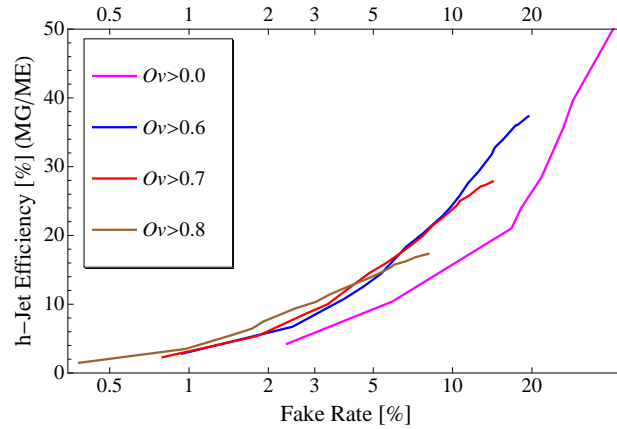


Figure 8: Fake rate *vs.* efficiency with various cuts on template overlap Ov and θ_s , for $R = 0.4$, $950 \text{ GeV} \leq P_0 \leq 1050 \text{ GeV}$, $110 \text{ GeV} \leq m_J \leq 130 \text{ GeV}$ and $m_H = 120 \text{ GeV}$. The curves are the result of varying the maximal value of θ_s . Both efficiency and fake rates decrease as we lower the cut on θ_s . (MG/ME [37] with MLM matching [38].)

the jet system. Therefore, we expect that planar flow for Higgs jets will be peaked toward a lower value than that of QCD jets.

In Fig. 9, on the upper left, we show the Pf distributions for QCD jet and Higgs jet events. This panel of the figure confirms our expectation that Higgs jets tend to have smaller Pf values than QCD jets events (for the same $z = m_J/P_0$). In the remaining panels, we show scatter plots of Pf vs. template overlap Ov , which show that both QCD and Higgs jets reflect two-pronged energy flow. In both cases, those events with large values of Ov tend to have relatively small values of Pf . We see, however, that the Higgs events yield somewhat smaller Pf , with a concentration of points at larger Ov in general, again in agreement with our heuristic expectations.

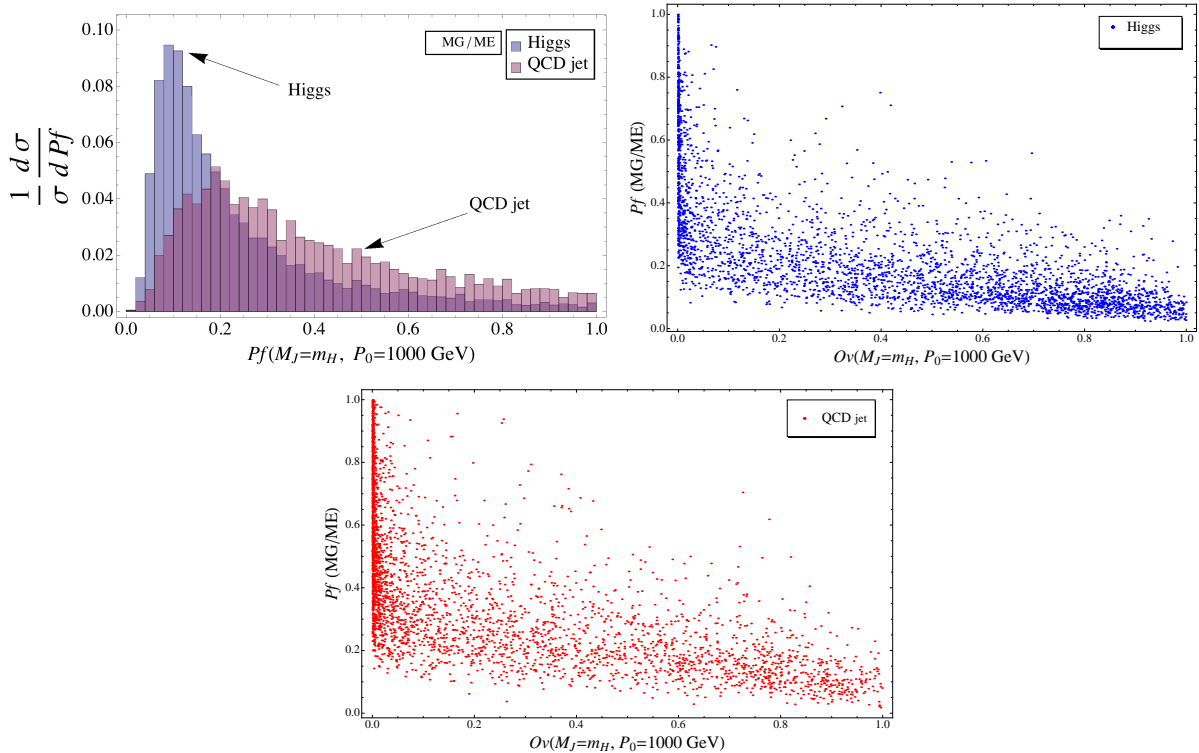


Figure 9: In the plot on the upper left, we show a histogram of Pf for Higgs jets and QCD jets. In the plot on the upper right, we show a scatter plot of Pf vs. template overlap Ov for Higgs jets. The remaining plot shows a scattering plot for QCD jets. Note the concentration of points for Higgs jets at larger values of Ov compared to QCD jets. We choose $R = 0.4$, $950 \text{ GeV} \leq P_0 \leq 1050 \text{ GeV}$, $110 \text{ GeV} \leq m_J \leq 130 \text{ GeV}$ and $m_H = 120 \text{ GeV}$. (MG/ME [37] with MLM matching [38])

Finally, in Fig. 10, we show the fake rate vs. efficiency when we combine template overlap, θ_s , and planar flow. In the plot on the right, we also show that angularities and θ_s indeed

have similar rejection powers. Once we combine the fake rate and efficiency from a jet mass cut (fake rate: 4.5%, efficiency: 79%) with template overlap, θ_s , and planar flow, we find, for example, at efficiency of 9.3%, a fake rate of 0.084% (with $Ov \geq 0.5$, $Pf \leq 0.09$, and $\theta_s \leq 0.2$).

Once again we point out that rejection power can be expected to improve once the template overlap is extended to take into account gluon emission. Another interesting but speculative aspect of our method is that, in principle, we can use the LEP data on Z decay and appropriately “boost” it to match for the relative kinematic regime to obtain an estimate of the all-orders template from the data itself.

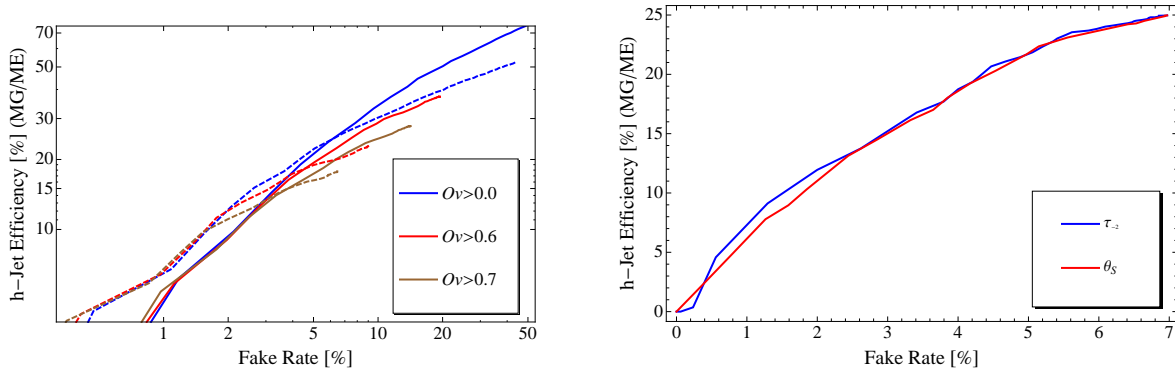


Figure 10: On the left (obtained via MG/ME [37] with MLM matching [38]), we show fake rate *vs.* efficiency, with various cuts of templates Ov , while varying the the value of Pf cut, corresponding to the change in efficiency. The dashed lines denote the case when $\theta_s \leq 0.2$ cut is implemented, while the solid lines have no θ_s cut. In the plot on the right, we show fake rate *vs.* efficiency with $Pf \leq 0.11$ and template overlap cut, $Ov \geq 0.1$, while varying the value of θ_s or angularity $\tilde{\tau}_{-2}$ cut, corresponding to the change in efficiency. We choose $R = 0.4$, $950 \text{ GeV} \leq P_0 \leq 1050 \text{ GeV}$, $110 \text{ GeV} \leq m_J \leq 130 \text{ GeV}$ and $m_H = 120 \text{ GeV}$.

5 Summary and Conclusions

Template overlaps are a new class of infrared safe jet observables, based on functional comparison of the energy flow in data with the flow in selected sets (the templates) of partonic states. We have demonstrated how, even with a relatively naive construction for the functional, template overlaps can be used to enrich samples of highly boosted particle decays in the presence of much larger QCD backgrounds. We have illustrated the method using lowest-order template states for highly-boosted Higgs and top decays, compared to the outputs of several event generators. This method, however, relies only on the infrared safety of energy flow, and is more general than boosted particle decay and may find other applications.

Different event generators give different averages for our template overlaps, which is

not surprising since the energy distributions within the jets are expected to be sensitive to the showering mechanism, which at present has not been tested experimentally for these kinematical configurations. We nevertheless find in each case excellent, although variable, rejection power, defined as the ratio between the signal efficiency and the background fake rate. For the Higgs jet case we get a rejection power of order 1:100 and for a single top jet of order 1:1000 (Pythia8), 1:600 (MG/ME), 1:200 (Sherpa) when combined with a jet mass cut, with sizable efficiencies. The fact that these rejection powers were found to be strong in all cases is encouraging. It also suggests that the template overlap method is robust, in the sense that it is not overly sensitive to the treatment of soft physics. The latter clearly varies between the different generators, which cannot all reproduce the coming LHC data. Differences may be due to treatments of multiple interactions, minimum bias and underlying events as well as showering mechanisms. The template overlaps described above are capable of systematic improvement by weighting according to the lowest order matrix elements (in different contexts, such an approach has been applied to Tevatron data [46]). We may also include higher order corrections in the template phase space. Other improvements may come from changing the functional that defines the overlap, or from more sophisticated cuts on the data.

Acknowledgments: We thank Juan Maldacena for very stimulating discussions. We also appreciate the efforts of Steffen Schumann to provide customized Sherpa cut for high P_T QCD and top jet generation. GP is the Shlomo and Michla Tomarin career development chair; GP is supported by the Israel Science Foundation (grant #1087/09), EU-FP7 Marie Curie, IRG fellowship and the Peter & Patricia Gruber Award. The work of LA, GS and IS was supported in part by the National Science Foundation, grants PHY-0354776, PHY-0354822 and PHY-0653342, and the work of LA was also supported in part by U.S. DOE under contract No. DE-AC02-98CH10886.

References

- [1] J. M. Butterworth, J. R. Ellis and A. R. Raklev, JHEP **0705**, 033 (2007) [arXiv:hep-ph/0702150].
- [2] D. Benchekrone, C. Driouichi, A. Hoummada, SN-ATLAS-2001-001, ATL-COM-PHYS-2000-020, EPJ Direct 3, 1 (2001); J. M. Butterworth, B. E. Cox and J. R. Forshaw, Phys. Rev. D **65**, 096014 (2002) [arXiv:hep-ph/0201098].
- [3] J. M. Butterworth, A. R. Davison, M. Rubin and G. P. Salam, Phys. Rev. Lett. **100**, 242001 (2008) [arXiv:0802.2470 [hep-ph]].
- [4] J. M. Butterworth, J. R. Ellis, A. R. Raklev and G. P. Salam, Phys. Rev. Lett. **103**, 241803 (2009) [arXiv:0906.0728 [hep-ph]].

- [5] K. Agashe, A. Belyaev, T. Krupovnickas, G. Perez and J. Virzi, Phys. Rev. D **77**, 015003 (2008) [arXiv:hep-ph/0612015].
- [6] B. Lillie, L. Randall and L. T. Wang, JHEP **0709**, 074 (2007) [arXiv:hep-ph/0701166].
- [7] A. L. Fitzpatrick, J. Kaplan, L. Randall and L. T. Wang, JHEP **0709**, 013 (2007) [arXiv:hep-ph/0701150].
- [8] K. Agashe, H. Davoudiasl, G. Perez and A. Soni, Phys. Rev. D **76**, 036006 (2007) [arXiv:hep-ph/0701186].
- [9] B. Lillie, J. Shu and T. M. P. Tait, Phys. Rev. D **76**, 115016 (2007) [arXiv:0706.3960 [hep-ph]].
- [10] K. Agashe *et al.*, Phys. Rev. D **76**, 115015 (2007) [arXiv:0709.0007 [hep-ph]].
- [11] T. Han, S.J. Lee, F. Maltoni, G. Perez, Z. Sullivan, T.M.P. Tait and L. T. Wang, in P. Nath *et al.*, Nucl. Phys. Proc. Suppl. **200-202**, 185 (2010) [arXiv:1001.2693 [hep-ph]].
- [12] S. Fleming, A. H. Hoang, S. Mantry and I. W. Stewart, arXiv:0711.2079 [hep-ph]; S. Fleming, A. H. Hoang, S. Mantry and I. W. Stewart, Phys. Rev. D **77**, 074010 (2008) [arXiv:hep-ph/0703207]; A. H. Hoang and I. W. Stewart, arXiv:0808.0222 [hep-ph].
- [13] A. Banfi, G. P. Salam and G. Zanderighi, JHEP **0707**, 026 (2007) [arXiv:0704.2999 [hep-ph]].
- [14] S. D. Ellis, J. Huston, K. Hatakeyama, P. Loch and M. Tonnesmann, Prog. Part. Nucl. Phys. **60**, 484 (2008) [arXiv:0712.2447 [hep-ph]].
- [15] L. G. Almeida, S. J. Lee, G. Perez, I. Sung and J. Virzi, Phys. Rev. D **79**, 074012 (2009) [arXiv:0810.0934 [hep-ph]].
- [16] J. Thaler and L. T. Wang, JHEP **0807**, 092 (2008) [arXiv:0806.0023 [hep-ph]].
- [17] L. G. Almeida, S. J. Lee, G. Perez, G. Sterman, I. Sung and J. Virzi, Phys. Rev. D **79**, 074017 (2009) [arXiv:0807.0234 [hep-ph]].
- [18] D. E. Kaplan, K. Rehermann, M. D. Schwartz and B. Tweedie, Phys. Rev. Lett. **101**, 142001 (2008) [arXiv:0806.0848 [hep-ph]].
- [19] S. D. Ellis, A. Hornig, C. Lee, C. K. Vermilion and J. R. Walsh, arXiv:1001.0014 [hep-ph]; S. D. Ellis, C. K. Vermilion and J. R. Walsh, arXiv:0912.0033 [hep-ph]; S. D. Ellis, C. K. Vermilion and J. R. Walsh, Phys. Rev. D **80**, 051501 (2009) [arXiv:0903.5081 [hep-ph]].
- [20] D. Krohn, J. Thaler and L. T. Wang, JHEP **1002**, 084 (2010) [arXiv:0912.1342 [hep-ph]].

- [21] G. D. Kribs, A. Martin, T. S. Roy and M. Spannowsky, arXiv:0912.4731 [hep-ph].
- [22] S. Chekanov and J. Proudfoot, arXiv:1002.3982 [hep-ph].
- [23] D. E. Soper and M. Spannowsky, arXiv:1005.0417 [hep-ph].
- [24] C. L. Basham, L. S. Brown, S. D. Ellis and S. T. Love, Phys. Rev. Lett. **41**, 1585 (1978).
- [25] N. A. Sveshnikov and F. V. Tkachov, Phys. Lett. B **382**, 403 (1996) [arXiv:hep-ph/9512370].
- [26] G. P. Korchemsky, G. Oderda and G. Sterman, arXiv:hep-ph/9708346, talk presented at 5th International Workshop on Deep Inelastic Scattering and QCD (DIS 97), Chicago, IL, 14-18 Apr 1997.
- [27] C. Lee and G. Sterman, Phys. Rev. D **75**, 014022 (2007) [arXiv:hep-ph/0611061]; C. W. Bauer, S. P. Fleming, C. Lee and G. Sterman, Phys. Rev. D **78**, 034027 (2008) [arXiv:0801.4569 [hep-ph]].
- [28] D. M. Hofman and J. Maldacena, JHEP **0805**, 012 (2008) [arXiv:0803.1467 [hep-th]].
- [29] J. M. Maldacena, JHEP **0305**, 013 (2003) [arXiv:astro-ph/0210603].
- [30] ATLAS Detector and physics performance TDR, CERN-LHCC-99-14; CMS Physics and performance TDR, Volume II: CERN-LHCC-2006-021.
- [31] G. Sterman, Phys. Rev. D **19**, 3135 (1979).
- [32] Y. S. Lai and B. A. Cole, arXiv:0806.1499 [nucl-ex].
- [33] G. Sterman, Phys. Rev. D **17**, 2789 (1978).
- [34] M. Cacciari, G. P. Salam and G. Soyez, JHEP **0804**, 063 (2008) [arXiv:0802.1189 [hep-ph]].
- [35] J. Pumplin, D. R. Stump, J. Huston, H. L. Lai, P. M. Nadolsky and W. K. Tung, JHEP **0207**, 012 (2002) [arXiv:hep-ph/0201195].
- [36] T. Sjostrand, S. Mrenna and P. Skands, Comput. Phys. Commun. **178**, 852 (2008) [arXiv:0710.3820 [hep-ph]].
- [37] F. Maltoni and T. Stelzer, JHEP **0302**, 027 (2003) [arXiv:hep-ph/0208156]; T. Stelzer and W. F. Long, Comput. Phys. Commun. **81**, 357 (1994) [arXiv:hep-ph/9401258]. JHEP **0709**, 028 (2007) [arXiv:0706.2334 [hep-ph]].
- [38] M. L. Mangano, M. Moretti, F. Piccinini and M. Treccani, JHEP **0701**, 013 (2007) [arXiv:hep-ph/0611129].

- [39] T. Sjostrand, S. Mrenna and P. Skands, JHEP **0605**, 026 (2006) [arXiv:hep-ph/0603175].
- [40] T. Gleisberg, S. Hoche, F. Krauss, M. Schonherr, S. Schumann, F. Siegert and J. Winter, JHEP **0902**, 007 (2009) [arXiv:0811.4622 [hep-ph]].
- [41] S. Hoeche, F. Krauss, S. Schumann and F. Siegert, JHEP **0905**, 053 (2009) [arXiv:0903.1219 [hep-ph]].
- [42] G. P. Salam, arXiv:0906.1833 [hep-ph].
- [43] C. F. Berger, T. Kucs and G. Sterman, Phys. Rev. D **68**, 014012 (2003) [arXiv:hep-ph/0303051]; C. F. Berger and L. Magnea, Phys. Rev. D **70**, 094010 (2004) [arXiv:hep-ph/0407024].
- [44] I. Sung, Phys. Rev. D **80**, 094020 (2009) [arXiv:0908.3688 [hep-ph]].
- [45] J. Gallicchio and M. D. Schwartz, arXiv:1001.5027 [hep-ph].
- [46] T. Aaltonen *et al.* [The CDF Collaboration], Phys. Rev. D **81**, 052011 (2010) [arXiv:1002.0365 [hep-ex]].